Dephasing in Strongly Anisotropic Black Phosphorus

Francesca Telesio

Pisa, 20/04/2017

National Enterprise for nanoScience and nanoTechnology

Summary

- Introduction: black Phosphorus
- Dephasing in black Phosphorus
  - Weak localization measurements
  - Data analysis and interpretation
  - Conclusions
- Other activites and outlooks:
  - bP functionalization with nanoparticles for catalysis applications
  - Alternative preparation methods for «cheap» few layer bP production: exfoliation trough MMA intercalation and poymerization
  - SEED project 2017: STM on exfoliated black Phosphorus

The family of phosphorus alloys

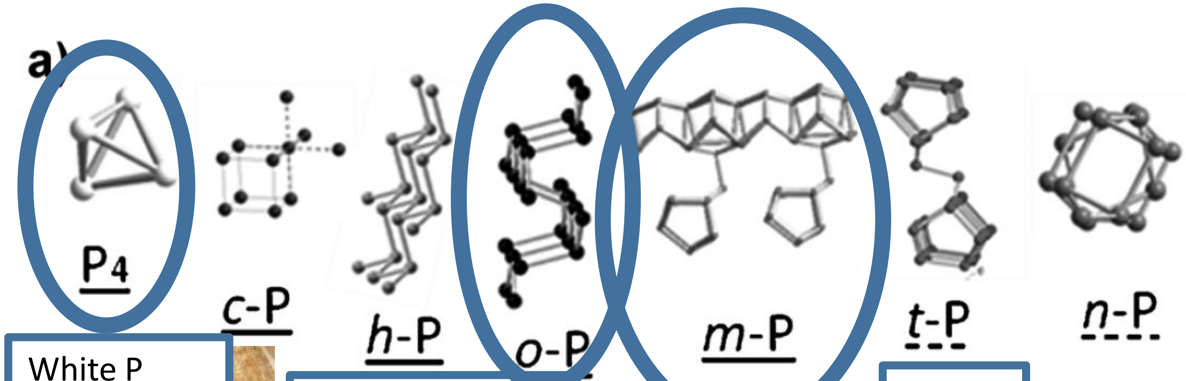

White P


Red P
(amorphous)


Black P
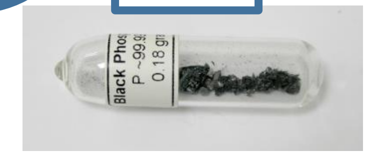

Violet P


Black phosphorus

2007, new synthesis method

12000 bar

White phosphorus

Red phosphorus

Violet phosphorus

Over 280°C

1-2 weeks over 550°C

pressure

temperature

F. Bachhuber et al., Angew. Chem. Int. Ed. 53 (2014) 11629

Black phosphorus

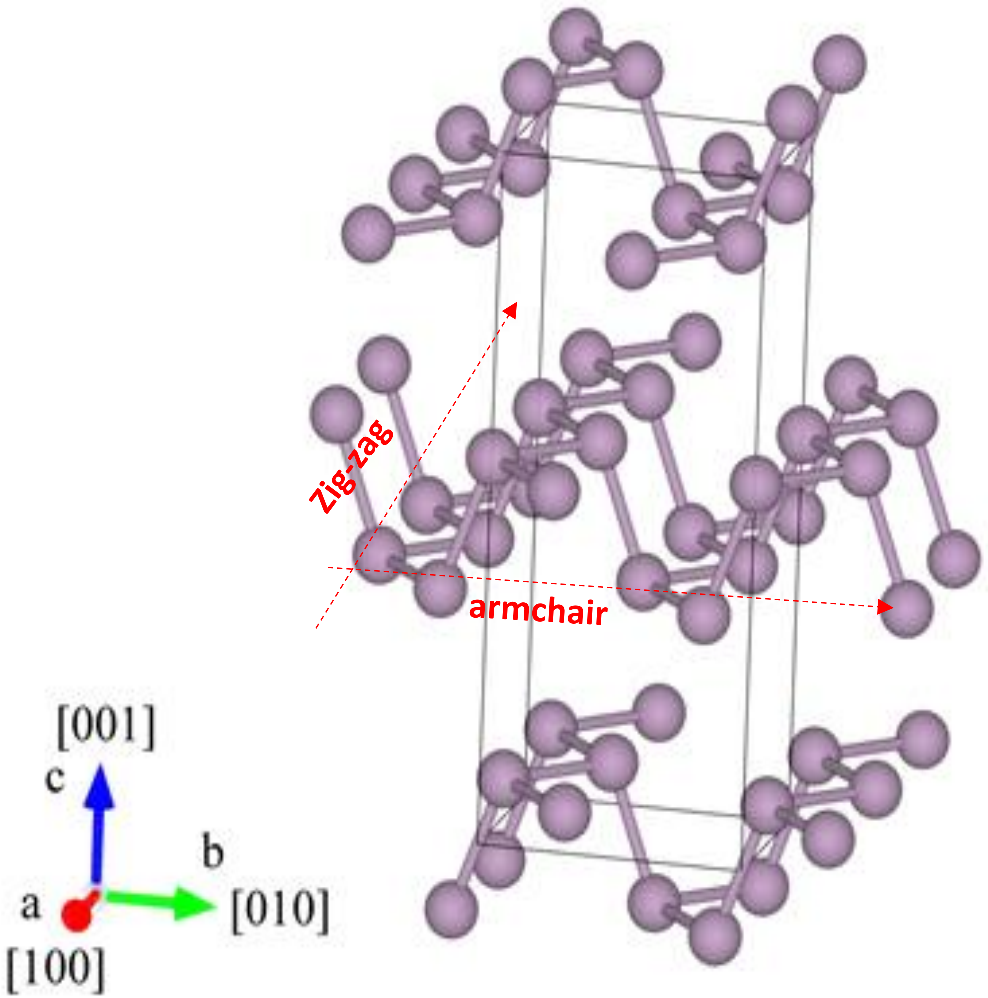

Cell parameters
a=3.13Å
b=10.47Å
c=4.37Å

A. Morita, Appl. Phys. A 39 (1986) 227

Black phosphorus

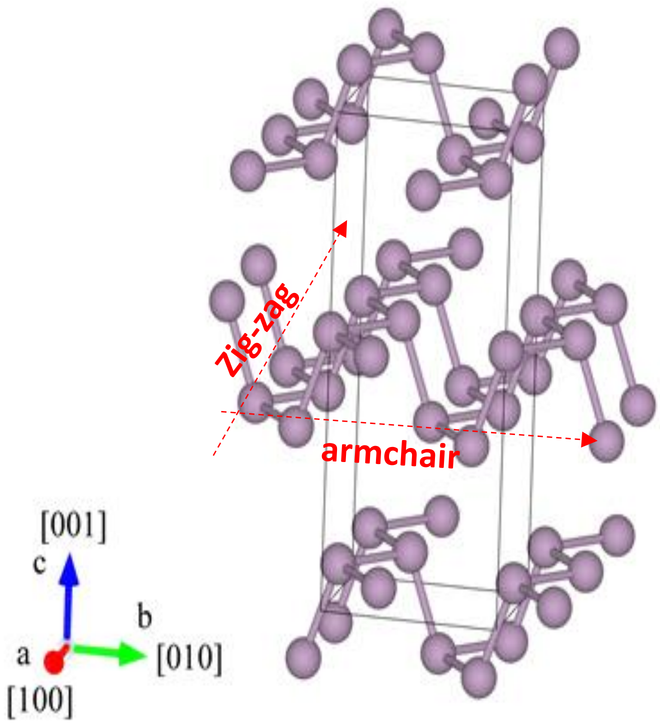

Cell parameters
a=3.13Å
b=10.47Å
c=4.37Å

- ✓In 1914 first successful synthesis (Bridgman) and in 2007 synthesis at room pressure (Lange, Nilges)
- ✓p-type semiconductor: 0.3eV direct band gap and high hole mobility (64,000 cm^2/Vs @ 20 K)
- ✓1983 (Narita): n-type doping by Te

A. Morita, Appl. Phys. A 39 (1986) 227

The Renaissance of Black Phosphorus

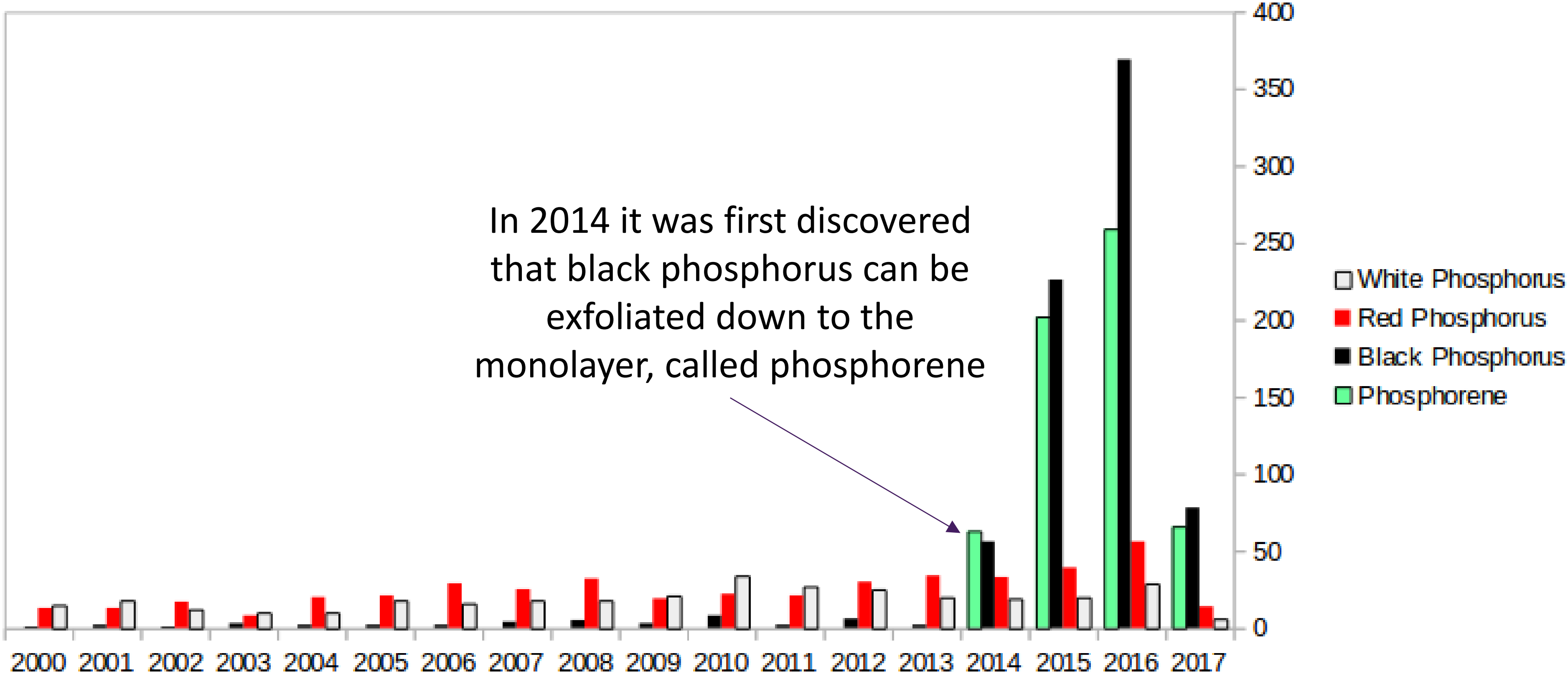

The renaissance of black phosphorus

- ✓Highly reactive in air
- ✓Direct band gap
- ✓Band-gap tunable with layer number
- ✓And much more... such as some recent measurements of quantum Hall effect at high field

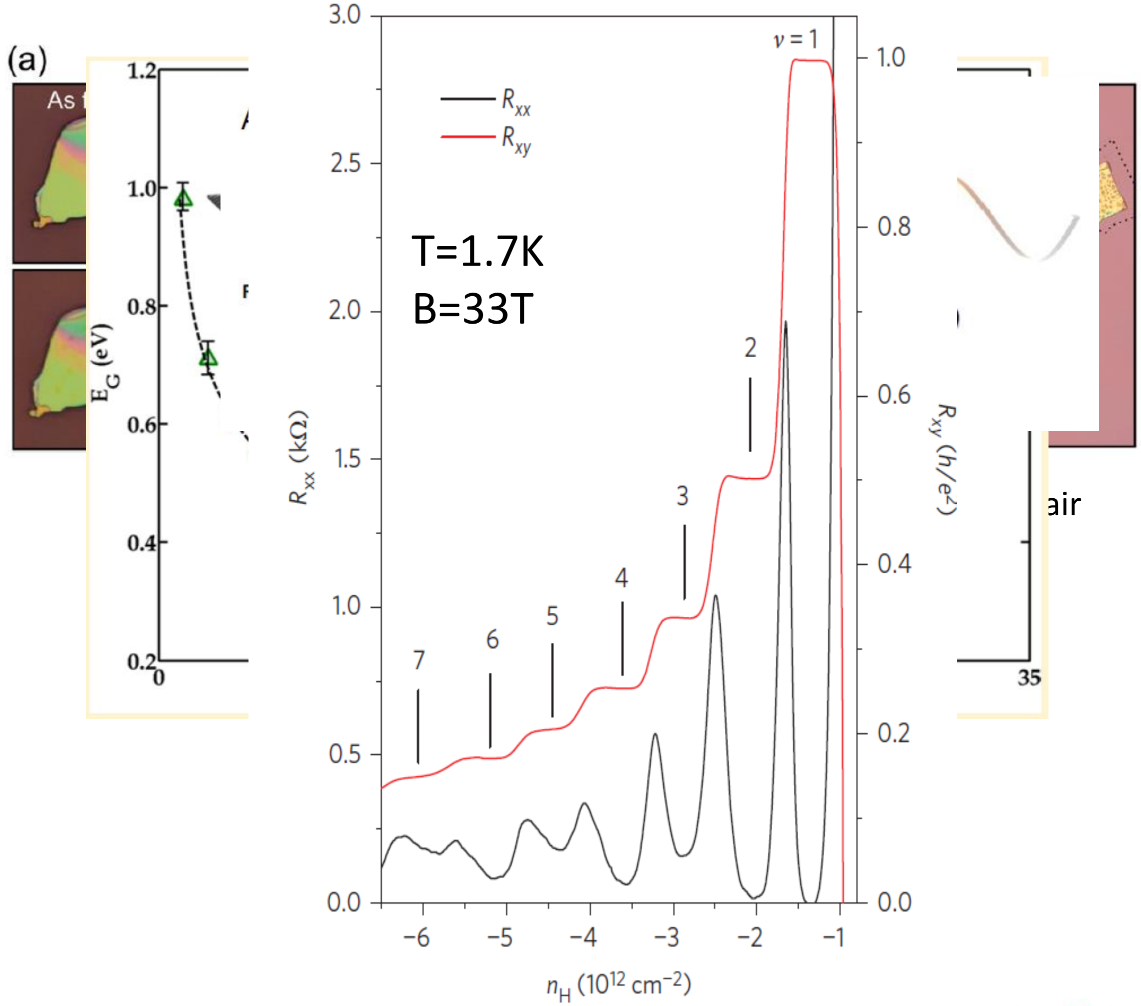

A. Castellanos-Gomez et al., 2D Mater. 1 (2014) 025001   S. Das et al., Nano Lett. 14 (2014) 5733

X. Ling et al., PNAS 112 (2015) 4523   L. Li et al., Nat. Nanotech 11 (2016), 593

The reinassance of black phosphorus

✓ **In-plane anisotropy** of optical and transport properties

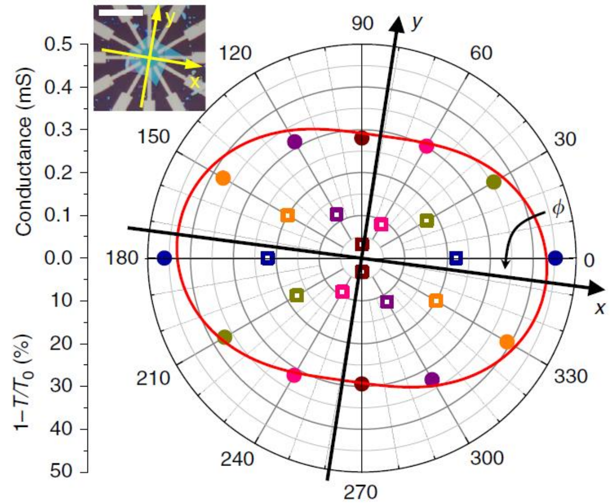

$\sigma_x/\sigma_y \approx 1.5$

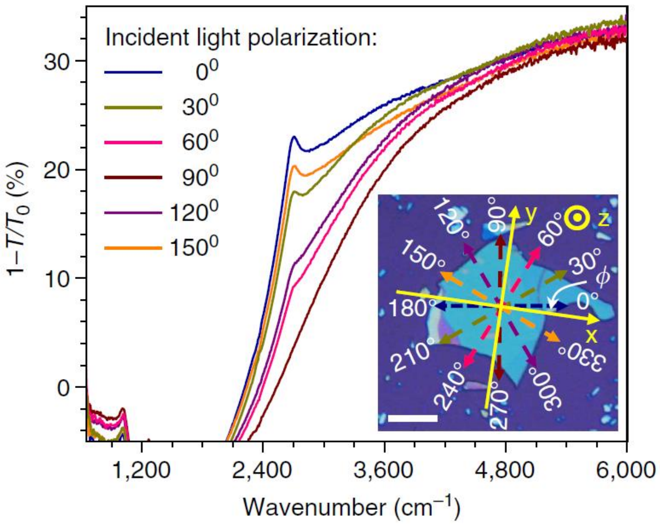

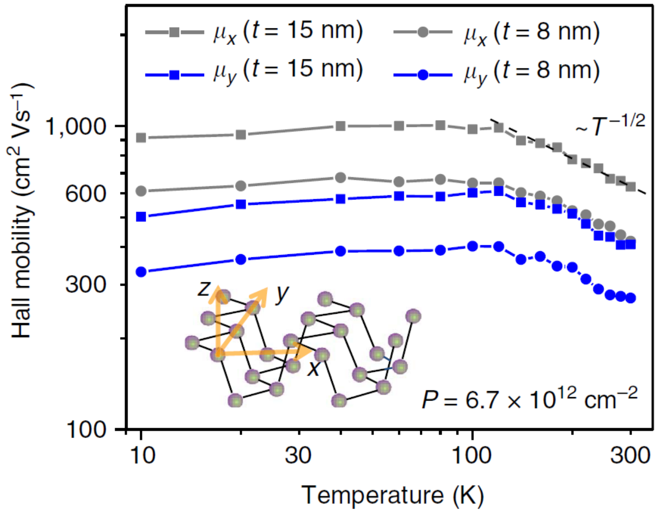

$\mu_x/\mu_y \approx 1.8$

F. Xia et al., Nat. Comm. 5 (2014) 4458

bP Field Effect Transistor

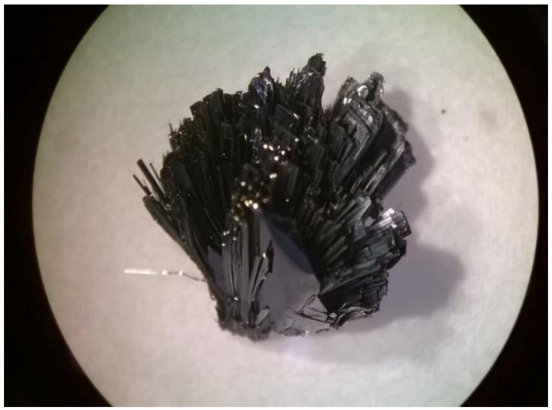

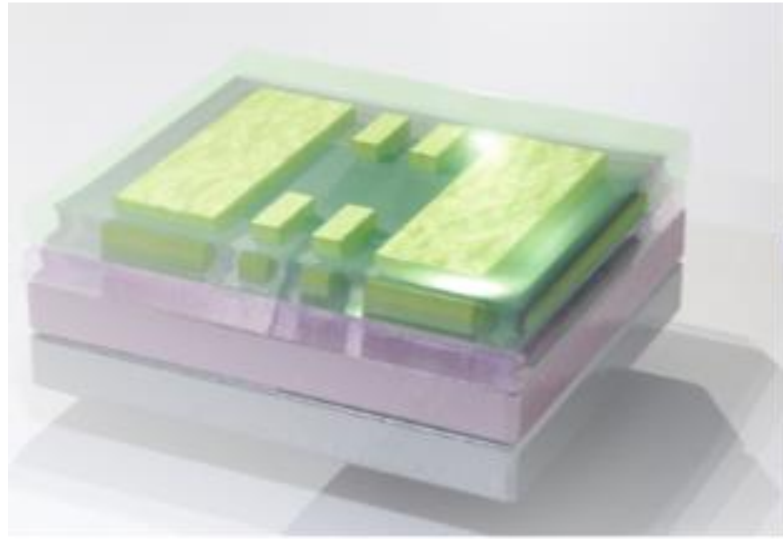

PMMA
MMA
Ti/Au contacts
bP flake
HMDS
SiO_2 thermal oxide
Si

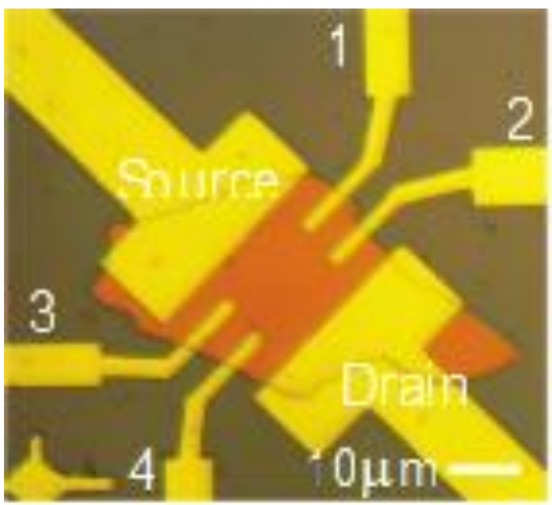

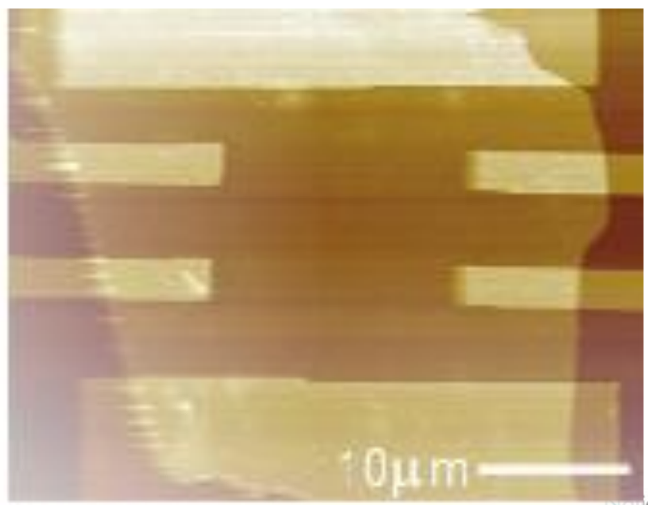

R_{xx}: 1-2
R_{xy}: 1-3

Flake thickness:
65 ± 2 nm

N.Hemsworth et al, PRB 94, 245404, (2016)

Transport Characterization

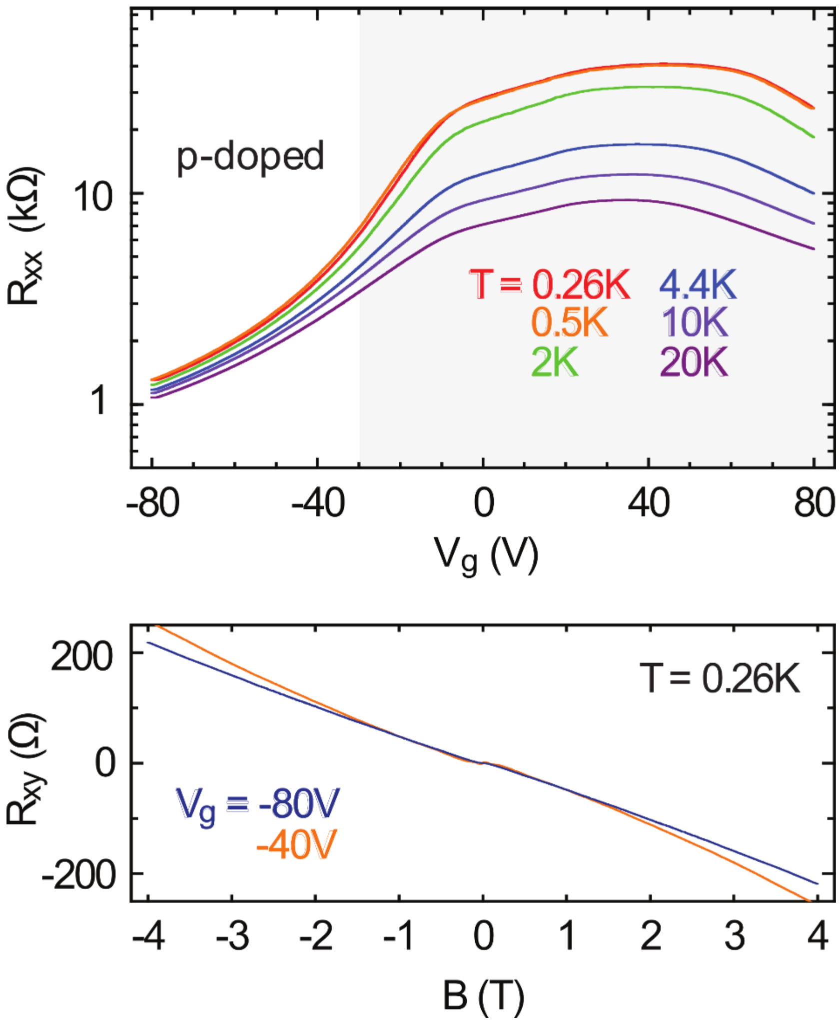

- p type for $V_g < -30$ V
- p = 10^{13} cm^{-2} for $V_g = -30$ V
- Field-effect mobility μ: 300 cm^2/Vs at $V_g = -70$ V
- Negligible T-dependence in μ for 0.26 K < T < 20 K

N.Hemsworth et al, PRB 94, 245404, (2016)

Longitudinal magnetotransport measurements

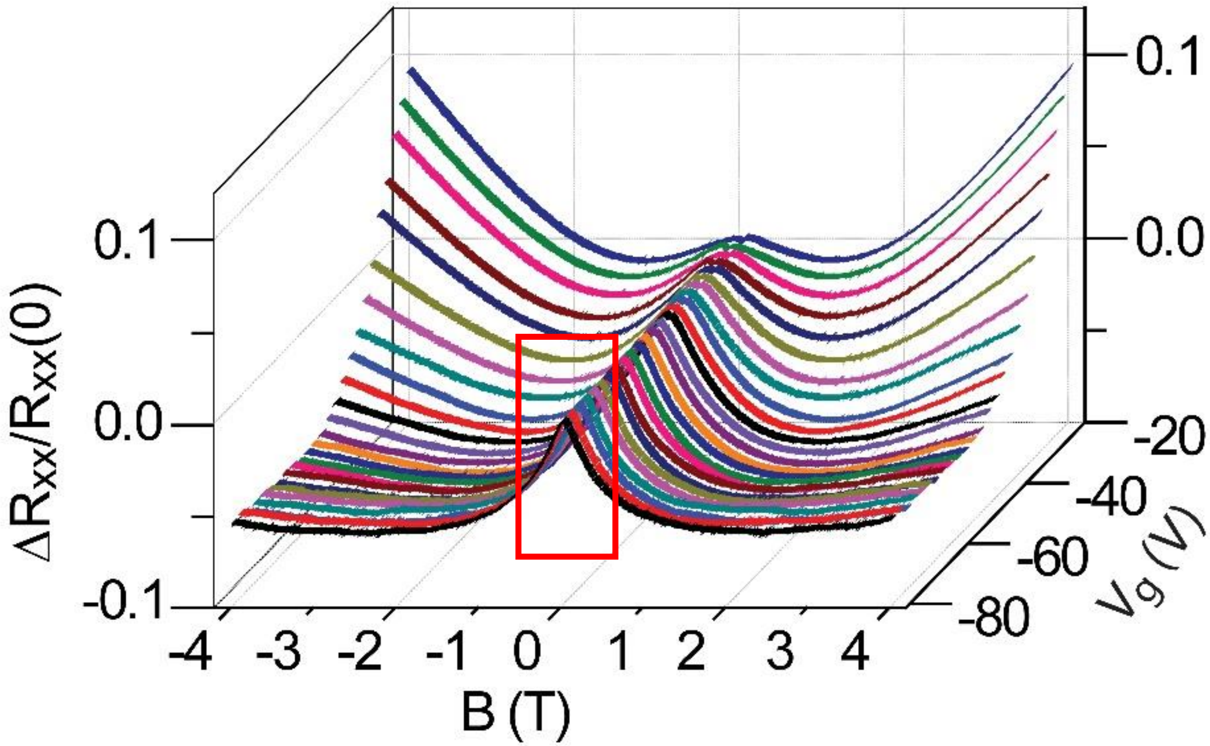

N.Hemsworth et al, PRB 94, 245404, (2016)

National Enterprise for nanoScience and nanoTechnology

Weak Localization

Weak localization is a quantum effect related to coherent scattering at low temperatures.

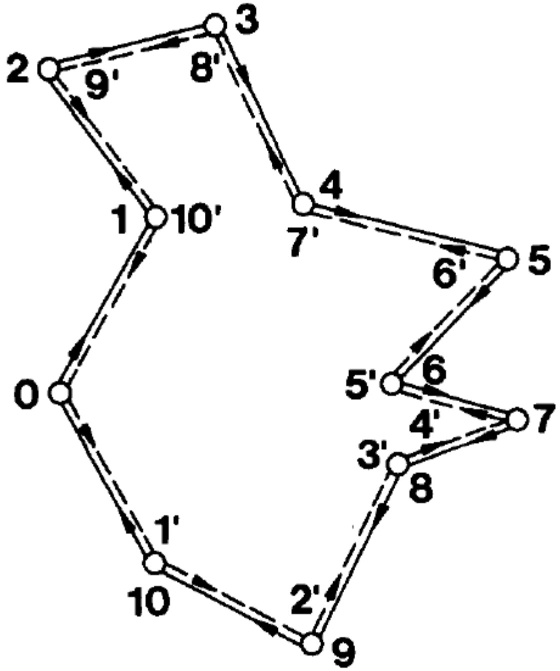

Picture from Bergmann, Weak localization in thin films, Physics Reports 107, 1984

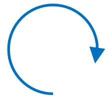 Amplitude A_1 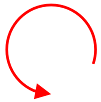 Amplitude A_2

Normal Diffusion Model:

$$P = |A_1|^2 + |A_2|^2 = 2\ |A|^2$$

Coherent Addition:

$$P = |A_1 + A_2|^2 = |2\ A|^2 = 4\ |A|^2$$

Since weak localization is a coherent scattering effect:

- It’s depressed by magnetic field
- It’s smeared by temperature

Weak Localization: Hikami-Larkin-Nagaoka model

NEST

McGill UNIVERSITY

$$\Delta\sigma = -\frac{e^2}{2\pi^2\hbar}\left(\Psi\left(\frac{1}{2}+\frac{B_1}{B}\right) - \frac{3}{2}\Psi\left(\frac{1}{2}+\frac{B_2}{B}\right) + \frac{1}{2}\Psi\left(\frac{1}{2}+\frac{B_3}{B}\right)\right)$$

Where Ψ is the digamma function

$$B_1 = B_0 + B_{so} + B_s$$

$$B_2 = \frac{4}{3}B_{so} + \frac{2}{3}B_s + B_\phi$$

$$B_3 = 2B_s + B_\phi$$

S. Hikami, A. I. Larkin, and Y. Nagaoka,
Prog. Of Theor. Phys. 63 (1980) 707.

Weak Localization

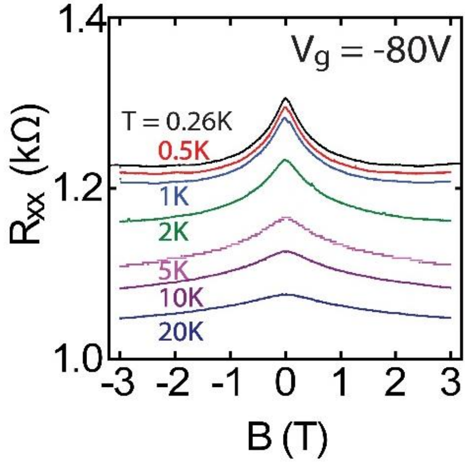

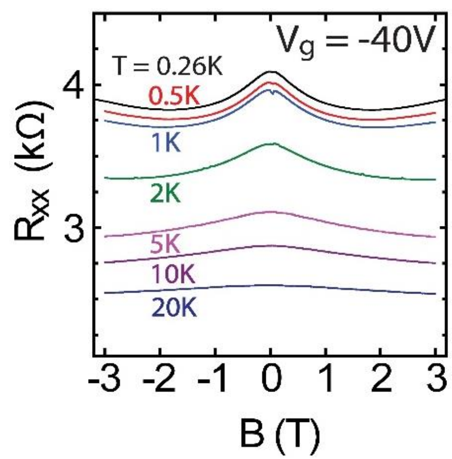

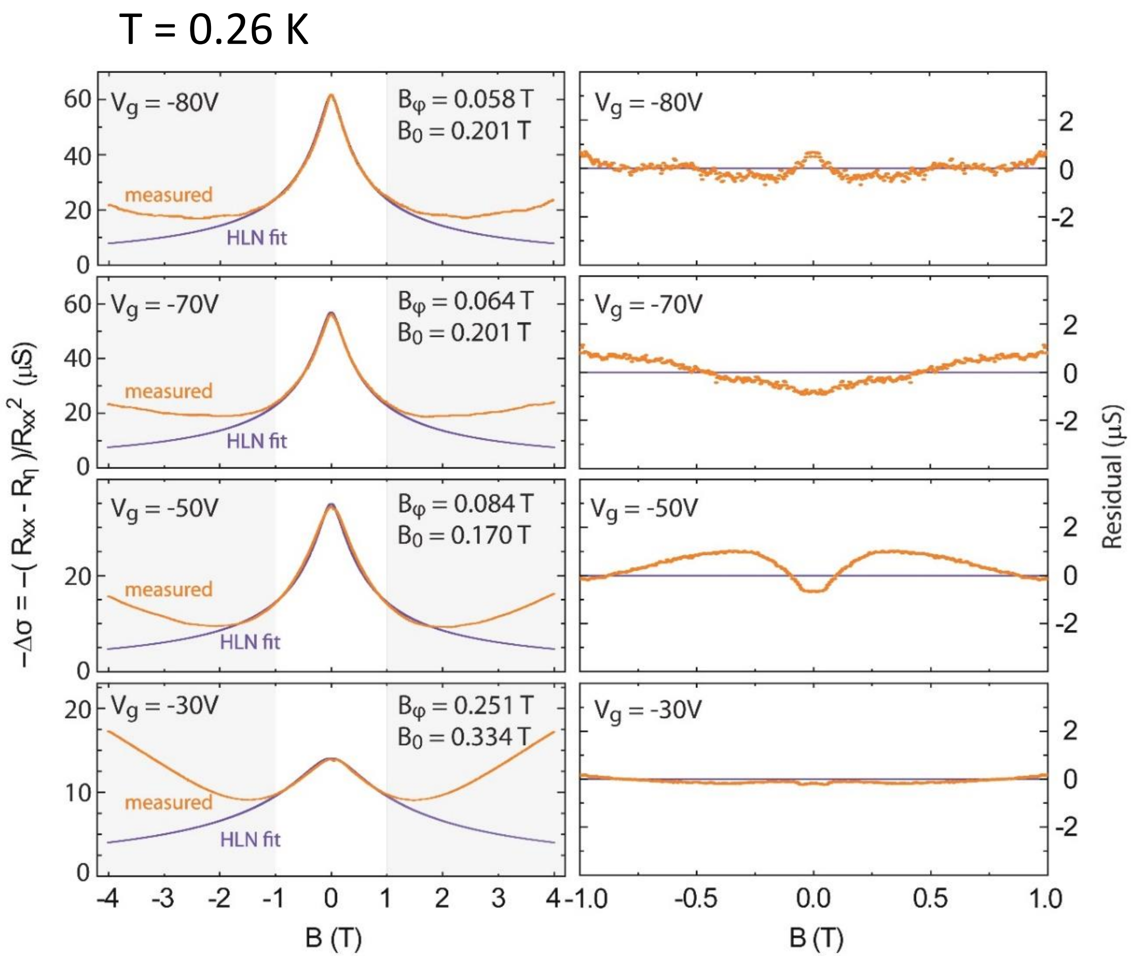

N.Hemsworth et al, PRB 94, 245404, (2016)

Scattering Lengths

$$BL^2 = {}^{h}/_{4e}$$

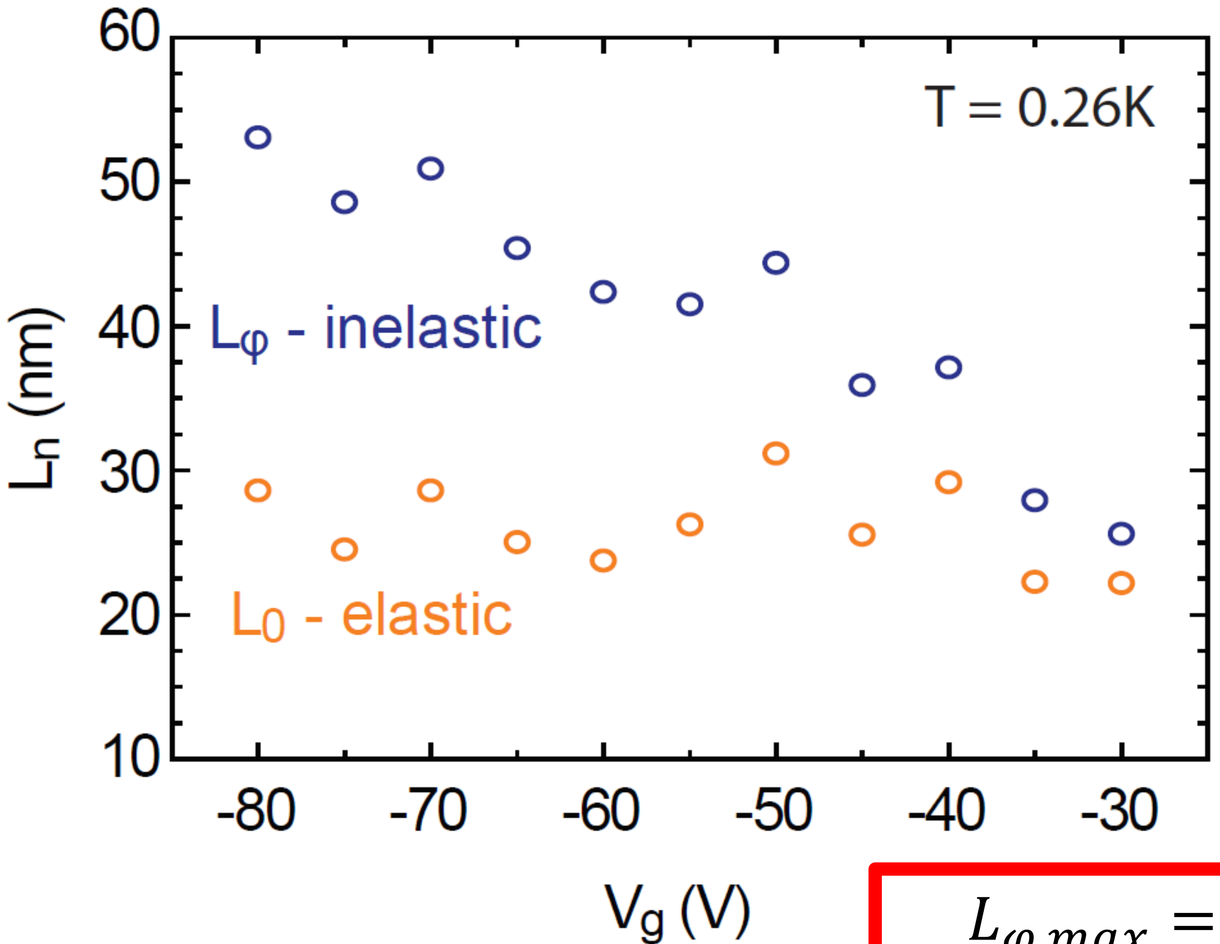

$$L_{\varphi,max} = 55\,nm$$

N.Hemsworth et al, PRB 94, 245404, (2016)

Scattering Lengths

- Ballistic transport: $\tau_\varphi \propto T^{-2}$
- Diffusive transport ($\tau_0 < \tau_\varphi$)

Dephasing length vs. inelastic scattering time: $L_\varphi = \sqrt{D\tau_\varphi}$ with *D* diffusion coefficient

$$\tau_\varphi \propto T^{-1} \text{ or } L_\varphi \propto T^{-1/2}$$

Lin and Bird, Jour. Phys. Cond. Mat. 14, R501, (2002)

National Enterprise for nanoScience and nanoTechnology

Scattering Lengths

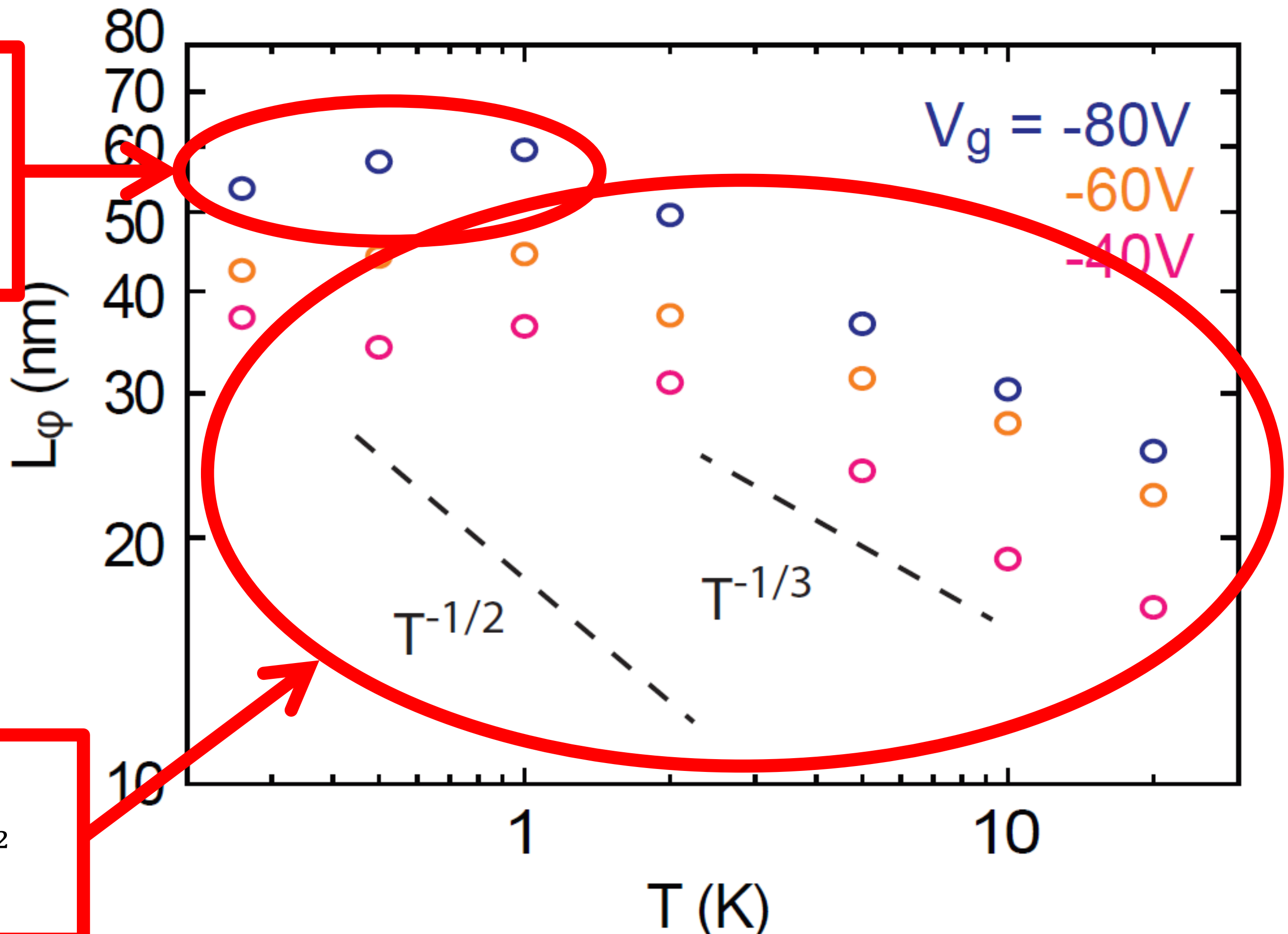

Saturation most likely due to impurities.

L_φ does not follow a $T^{-1/2}$ behaviour.

N.Hemsworth et al, PRB 94, 245404, (2016)

Qasi-1D systems

VOLUME 86, NUMBER 9 PHYSICAL REVIEW LETTERS 26 FEBRUARY 2001

Geometry-Dependent Dephasing in Small Metallic Wires

D. Natelson, R. L. Willett, K. W. West, and L. N. Pfeiffer
Bell Laboratories, Lucent Technologies, Murray Hill, New Jersey 07974
(Received 19 June 2000)

Temperature dependent weak localization is measured in metallic nanowires in a previously unexplored size regime down to width $w = 5$ nm. The dephasing time, τ_ϕ, shows a low temperature T dependence close to quasi-1D theoretical expectations ($\tau_\phi \sim T^{-2/3}$) in the narrowest wires, but exhibits a relative saturation as $T \to 0$ for wide samples of the same material, as observed previously. As only sample geometry is varied to exhib[...]
constraint on models of dephasing [...]

PHYSICAL REVIEW B, VOLUME 64, 121404(R)

Phase-coherent transport in ropes of single-wall carbon nanotubes

J. Appenzeller, R. Martel, and Ph. Avouris
IBM T. J. Watson Research Center, Yorktown Heights, New York 10598

H. Stahl, U. Th. Hunger, and B. Lengeler
II. Physikalisches Institut, RWTH Aachen, Templergraben 55, 52056 Aachen, Germany
(Received 21 May 2001; revised manuscript received 23 July 2001; published 6 September 2001)

To study the phase breaking scattering events in single-wall carbon nanotubes (SWNTs), ropes of SWNTs are intentionally damaged by Ar^+ ion milling. Due to this treatment, the average distance an electron can travel before being elastically scattered is reduced to about 10 nm. This significantly increases the probability of one-dimensional localization and allows us to obtain the phase coherence length (L_Φ) in ropes of SWNTs as a function of temperature. We find that Nyquist scattering ($\tau_\Phi \sim T^{-2/3}$) as well as another dephasing mechanism with a $\tau_\Phi \sim T^{-1}$ dependence are involved in limiting the phase-coherent transport. We also investigate the scattering of hot electrons in the system. The results support the statement that two different scattering mechanisms dominate the phase coherence length for different rope samples.

Comparison with quasi-1D wires

D. Natelson et al. PRL 86 (2009):

quasi-1D:

$L_\varphi, L_T > w, t$

width w
thickness t

$\tau_\varphi \propto T^{-2/3}$

$L_\varphi \propto T^{-1/3}$

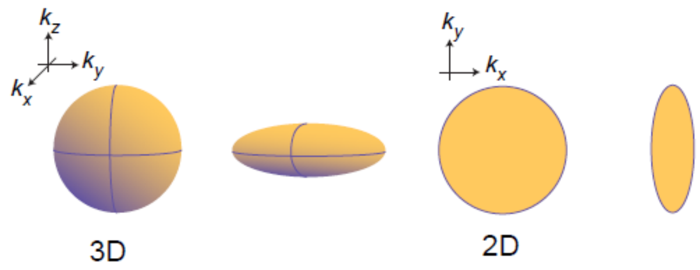

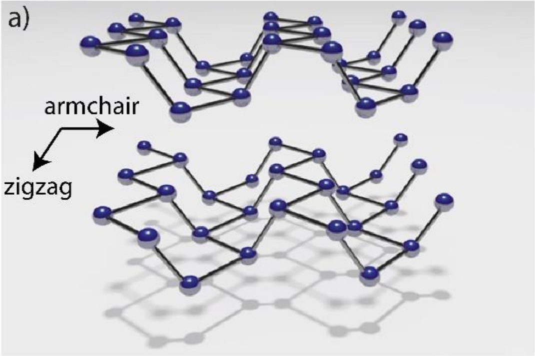

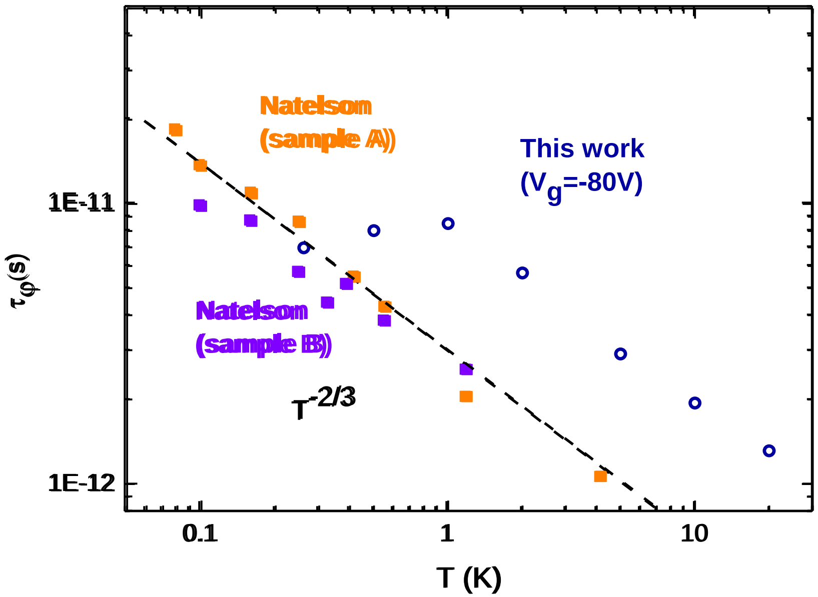

$L_\varphi = 55\ nm$

thermal length:

$L_T = \sqrt{\hbar D / k_B T}$ = 10 – 60 nm

N.Hemsworth et al, PRB 94, 245404, (2016)

Conclusions...

- ✓ Weak localization oberved in a bP FET
- ✓ Excellent agreement with HLN model
- ✓ Dephasing length L_φ reaches 55 nm
- ✓ T-dependence of L_φ close to quasi-1D
- ✓ This is a further proof of strong in plane anisotropy of bP

N.Hemsworth, et al, PRB 94, 245404, (2016)

Ongoing activities and outlooks/1: Decoration of 2D bP with Ni nanoparticles and applications in catalysis.

Florence

Liquid phase exfoliation of bP in DMSO, followed by functionalization with Ni nanoparticles.

a)

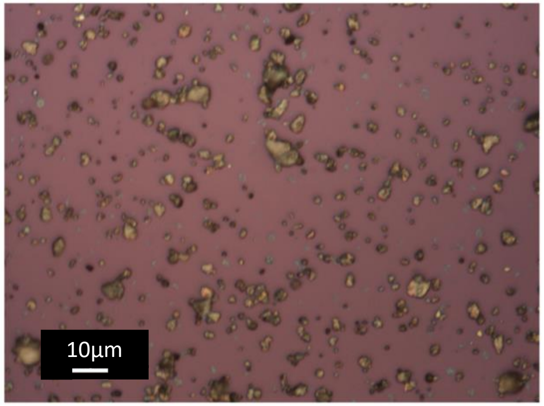

Optical microscopy

b)

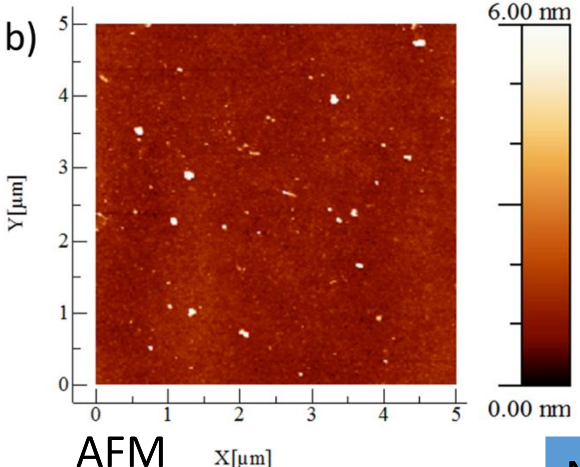

AFM

c)

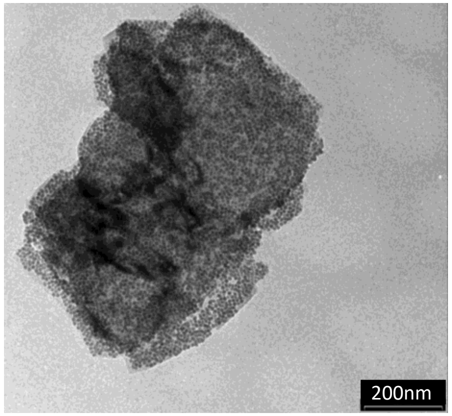

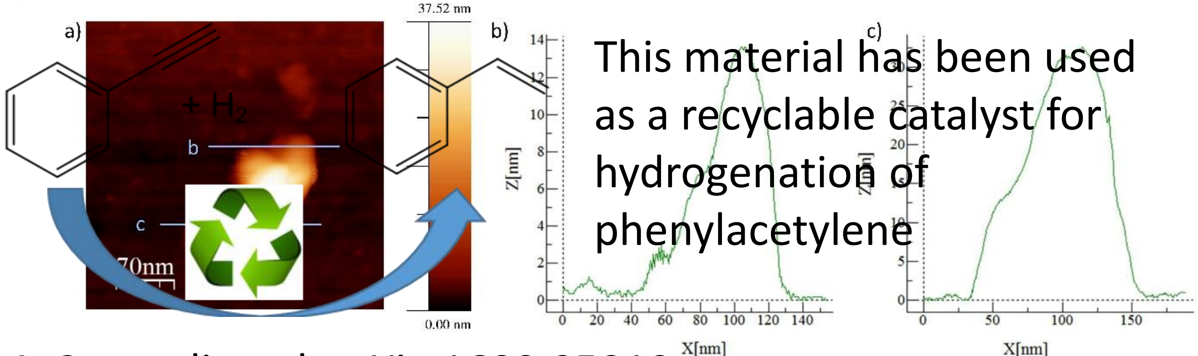

This material has been used as a recyclable catalyst for hydrogenation of phenylacetylene

Next steps:

- How this functionalization changes the properties of exfoliated bP?
- Can we functionalize mechanically exfoliated flakes?

M. Caporali et al, arXiv:1609.05010

Ongoing activities and outlooks/2: bP exfoliation by MMA intercalation and polymerization.

Pisa

From ICCOM Florence

Exfoliation
Ultrasonication

→

Polymer solution
PS or PMMA or PLA in $CHCl_3$

Polystyrene
PS/BP suspension
500/5 mg/mg

Poly(methyl)methacrylate
PMMA/BP suspension
500/5 mg/mg

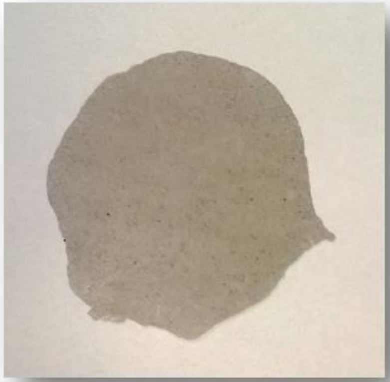

This blend is solved in anisole and then spinned at NEST.

Ongoing activities and outlooks/2: bP exfoliation by MMA intercalation and polymerization.

Pisa

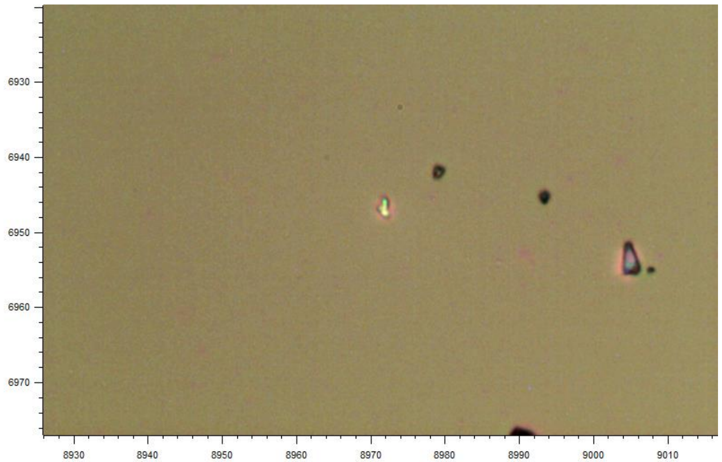

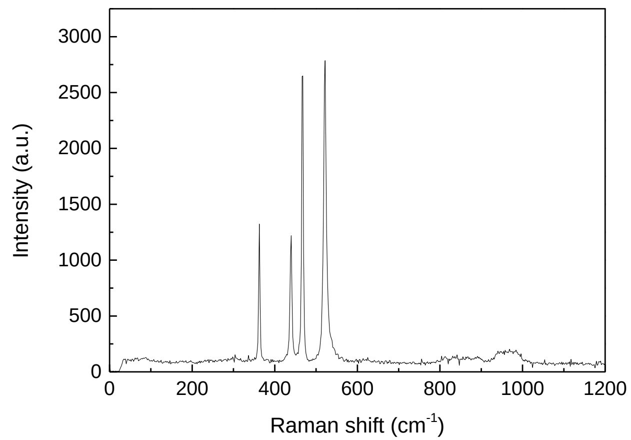

After spinning the blend, Raman active flake-like structure can be found but…

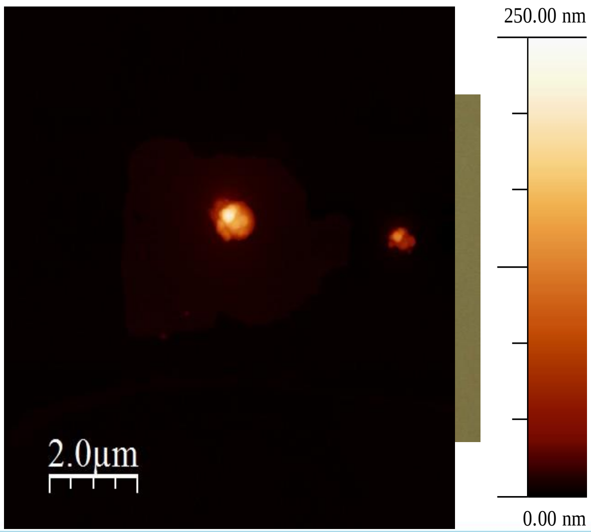

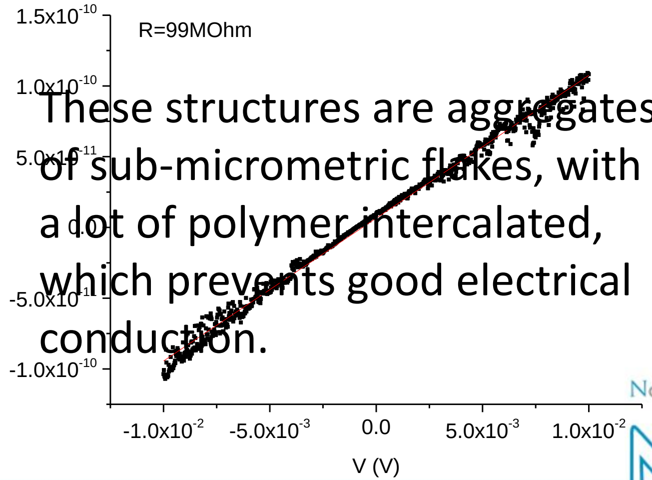

These structures are aggregates of sub-micrometric flakes, with a lot of polymer intercalated, which prevents good electrical conduction.

Ongoing activities and outlooks/3: SEED project.

SEED Project
SURface properties of few layer black PHOSphorus investigated by scanning tunnelling microscopy

- Clean surface of few-layer bP
  - On graphene on SiC
  - On Si/SiO_2
- Study of point defects
- Functionalization of the surface by metal evaporation

CNRNANO
ISTITUTO NANOSCIENZE CONSIGLIO NAZIONALE DELLE RICERCHE

National Enterprise for nanoScience and nanoTechnology
NEST

Ongoing activities and outlooks/3: SEED project.

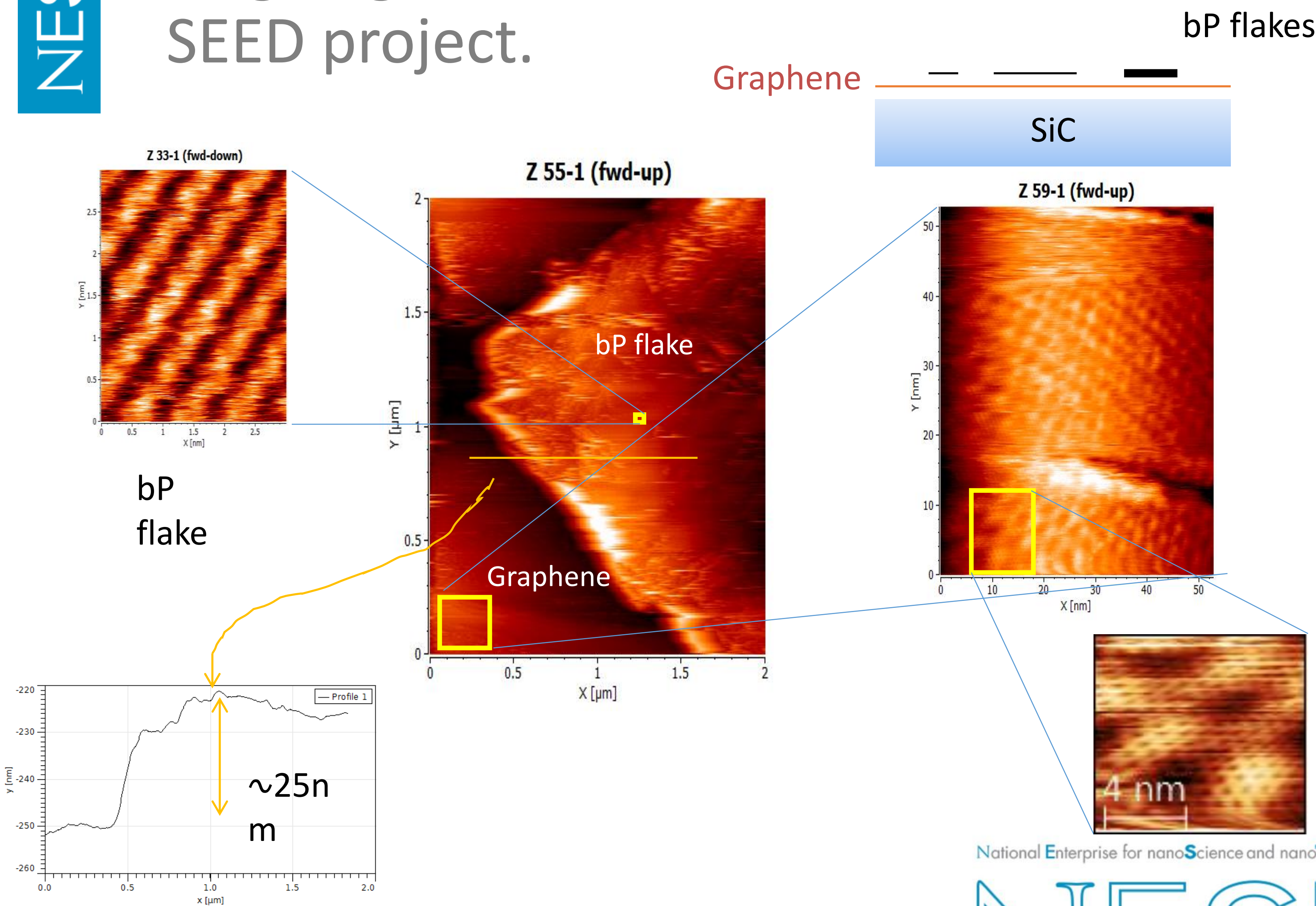

Ongoing activities and outlooks/3: SEED project.

Atomic Resolution on few-layer bP

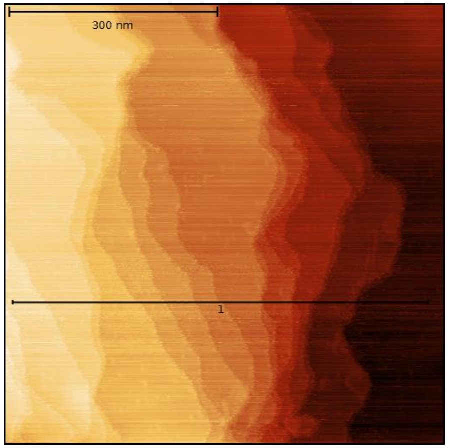

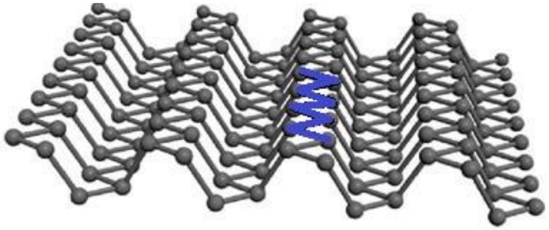

Morita, A et. al. Appl. Phys. A: Mater. Sci. Proc. 1986, 39, 227.

$$a = 3.313\ \text{Å}$$
$$b = 10.473\ \text{Å}$$
$$c = 4.374\ \text{Å}$$

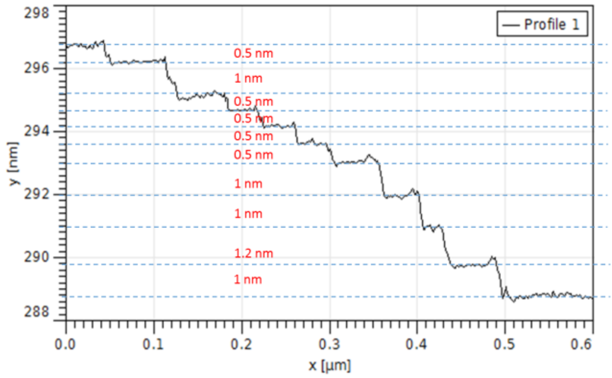

Measured at room temperature

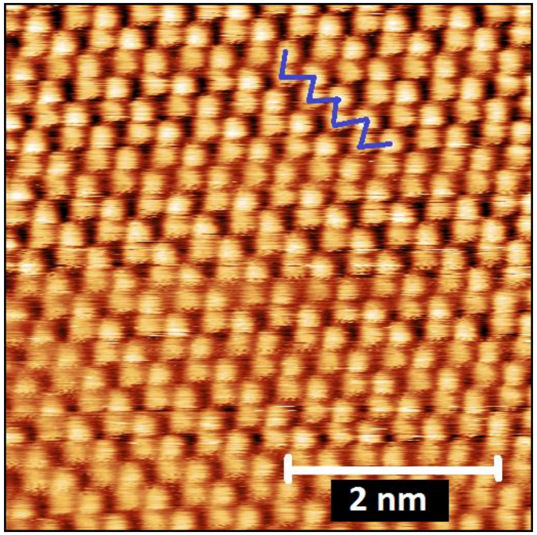

Measured unit cell parameter
a = 3.86 Å, c = 4.27 Å

Measured parameters are in very close agreement to the reported and predicted values.

Ongoing activities and outlooks/3: SEED project.

Controlled desorption of bP

Xiaolong Liu et. al., J. Phys. Chem. Lett. 2015, 6, 773.

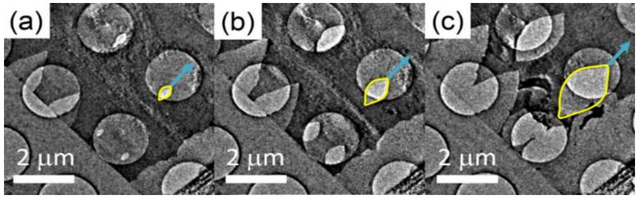

TEM image of eye shaped crack opening on heating bP flake at 400°C for 5, 8 and 12 min.

- decomposition of 2D BP is observed to occur at ~400 °C in vacuum, in contrast to the 550 °C bulk BP sublimation temperature
- This decomposition initiates via eye-shaped cracks along the [001] direction

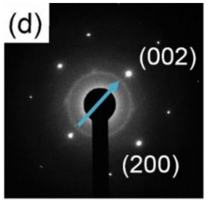

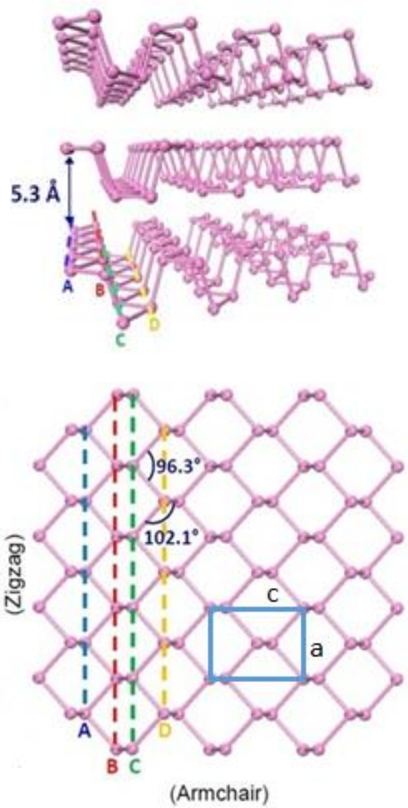

M. F. Deschenes et. al., J. Phys. Chem. Lett. 2016, 7, 1667.

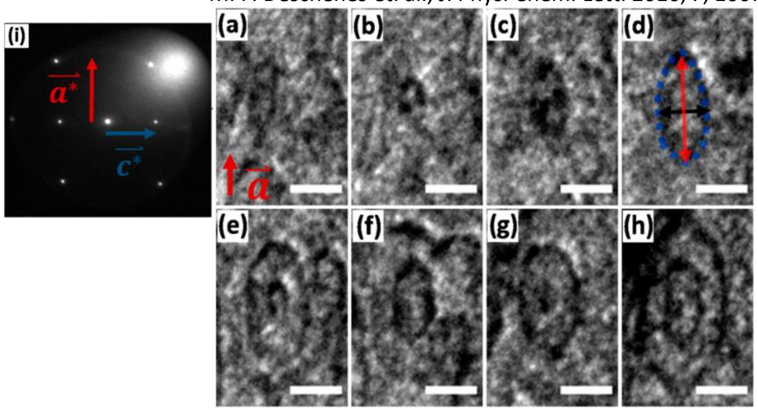

Bright-field LEEM snapshots of hole expansion during sublimation of exfoliated bP. Two seconds between each image from (a) to (h) recorded respectively at the following temperatures: 486 °C, 488 °C, 490 °C, 491 °C, 493 °C, 495 °C, 497 °C, and 499 °C.

- Sublimation manifests itself above 375 ± 20 °C
- Faceted holes with the long axis aligned along the [100] direction, in contrast to what was reported earlier

Ongoing activities and outlooks/3: SEED project.

- Sample annealed for 2 hours at temperatures in $50°C$ succession
- Couldn't see any flake at $550°C$ – most of them desorbs – leaving very low flake density
- Dashed line drawn in the plots below guides the decreasing flake width and height with temperature

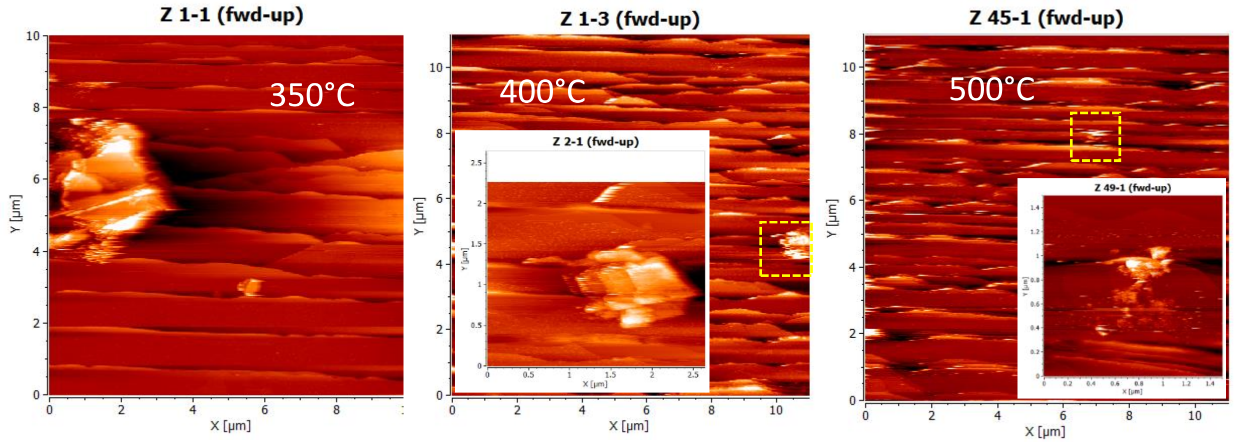

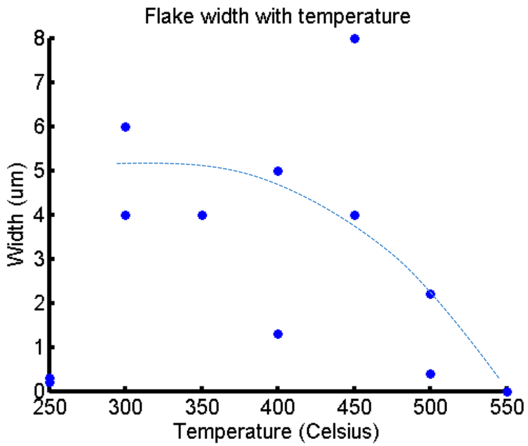

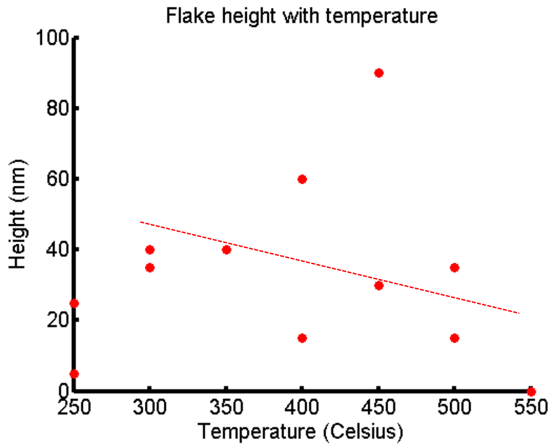

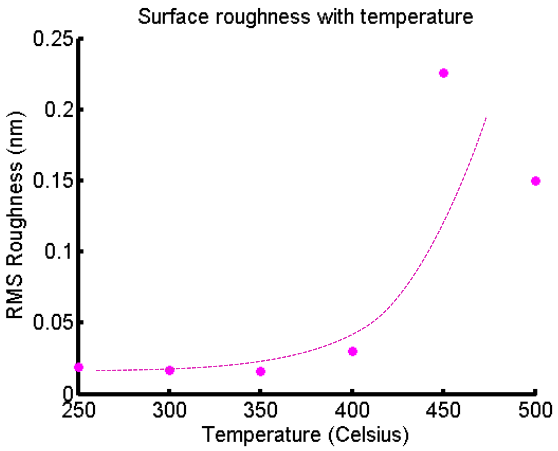

National Enterprise for nanoScience and nanoTechnology

Ongoing activities and outlooks/3: SEED project.

PRELIMINARY RESULTS!!

M. F. Deschenes et. al., J. Phys. Chem. Lett. 2016, 7, 1667.

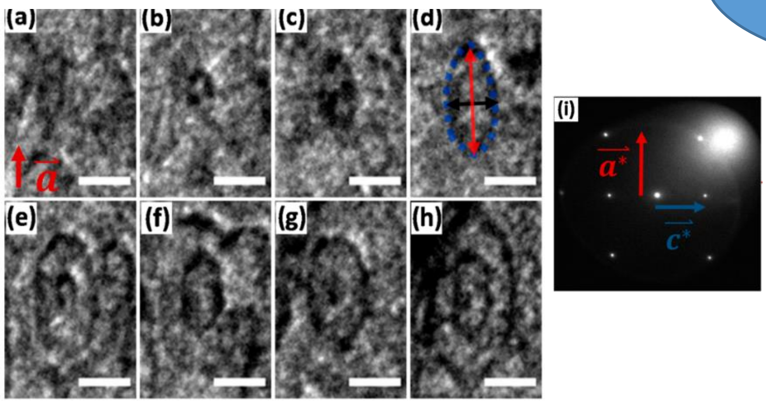

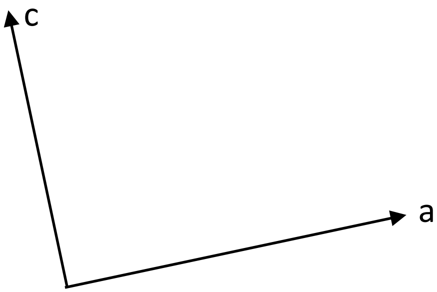

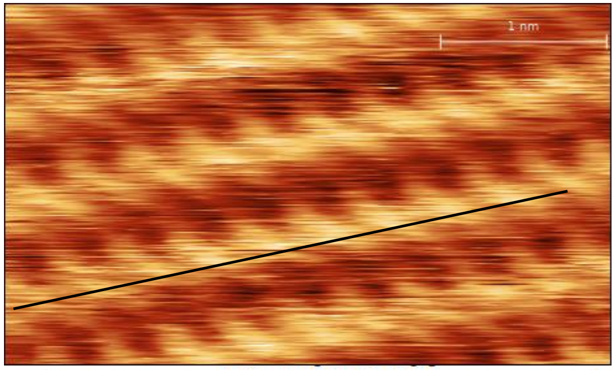

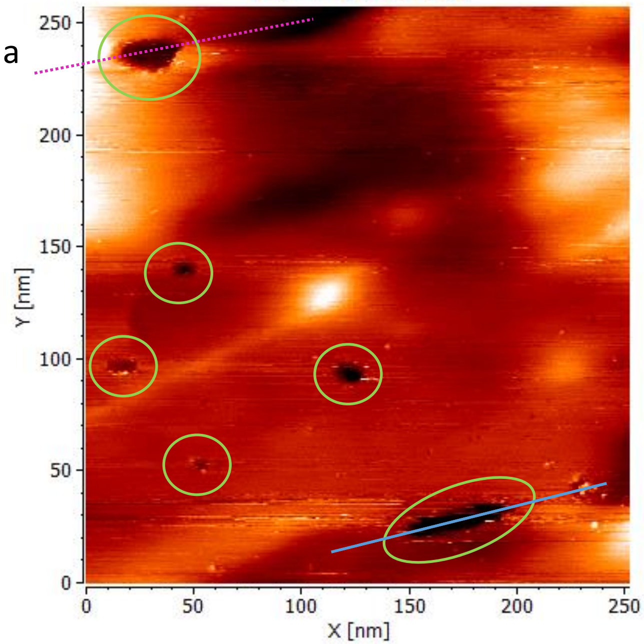

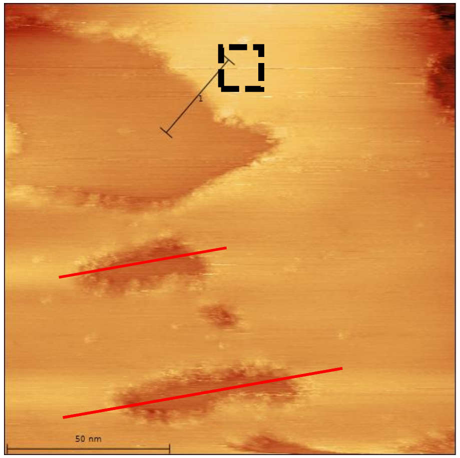

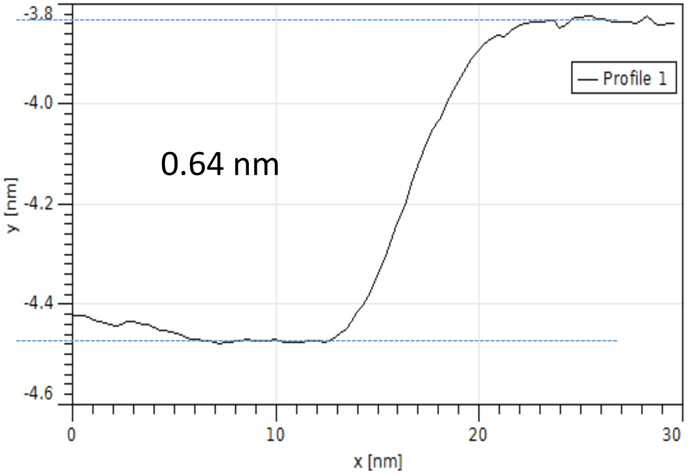

…further measurements are ongoing

National Enterprise for nanoScience and nanoTechnology


N. Hemsworth


V. Tayari


G. Gervais


T. Szkopek


S.Heun


S. Xiang


S. Roddaro


A. Kumar


D. Prezzi


M. Caporali


A. Ienco


M. Serrano-Ruiz


M. Peruzzini


E. Passaglia

*"**Phos**phorene **fun**ctionalization: a new platform for advanced multifunctional materials"*

*SEED Project : **Sur**face properties of black **Phos**phorus investigated by scanning tunneling microscopy*

Thank you for your attention!

National Enterprise for nanoScience and nanoTechnology

NEST